Yonsei Medical Journal
Vol. 38, No. 1, pp. 33~39, 1997

Hemodynamics of the Total Cavopulmonary Connection: An *in Vitro* Study

Sang Hyun Kim[1], Young Hwan Park[2], and Bum Ku Cho[2]

To understand the local fluid dynamics for different designs of Fontan operation, five models were made of Pyrex glass to facilitate in vitro study. Models I, II and III had the same position as the center of the anastomosis of the IVC (inferior vena cava) with that of the SVC (superior vena cava), but Models IV and V had 10 mm offset between them. As well, the anastomotic junction angles were different (Models I and IV: 90°, Models II and V: 70°, Model III: 45°). These models were then connected to a flow loop for flow visualization study. In Model I, no dominant vortex was seen in the central region of the junction, but a large unstable vortex was created in Models II and III. In Models IV and V, a significant stagnation region was created in the middle of the offset region. It also showed that the flow distribution from the IVC and SVC to the LPA (left pulmonary artery) and RPA (right pulmonary artery) depends more on the offset of the junction than on the anastomotic junction angle. Generally, as the total flow rates increased, the pressures in the models increased.

Key Words: Fontan operation, hemodynamics, flow visualization technique

Total cavopulmonary (CP) connection has been developed to treat hearts with essentially a single ventricular chamber (Fontan and Baudet, 1971). This includes hearts with one double inlet ventricle, biventricular hearts with hypoplasia of one ventricular chamber and left or right atrioventricular valve atresia. In a typical CP connection, the superior vena cava (SVC) and inferior vena cava (IVC) are connected directly to the right pulmonary artery (RPA). The blood flow in the operation is driven by a single ventricle bypassing the right heart. A high incidence of failures occurred due to fibromuscular ingrowth, valvular degeneration and pseudo intimal peel formation. All of which might depend on the hemodynamics of the connection through the presence of stasis, wall shear stress or energy loss due to the conduits. The energy loss is important because the right heart lost its pumping system, putting an increased workload on the left ventricle which then had to drive the blood through the lungs as well as through the rest of the body. In terms of local fluid dynamics, the surgically-created circuit should not cause blood-flow abnormalities.

Many post-operative clinical studies were conducted to observe the blood flow in Fontan patients, mainly using echocardiography (Nakazawa *et al.* 1987; Frommelt *et al.* 1991; Kobayashi *et al.* 1991; Penny and Redington, 1991) and MRI (Rebergen *et al.* 1993). There has been very little in vitro study on the hemodynamics of the CP connection (de Leval

Received December 16, 1996
Accepted February 28, 1997
Cardiovascular Research Institute[1] and Department of Cardiovascular Surgery[2], Yonsei University College of Medicine, Seoul 120-752, Korea
This research was supported by a faculty research grant of Yonsei Cardiovascular Research Institute and Woonkyung foundation (1995).
Address reprint request to Dr. S.H. Kim, Cardiovascular Research Institute, Yonsei University College of Medicine, Seoul 120-752, Korea

et al. 1988; Low *et al.* 1992; Kim *et al.* 1995; Dubini *et al.* 1996). Although these studies help to understand the hemodynamics of the CP connection, it is often difficult to make comparisons because of the differences in model geometry, flow rates and the position of measurement. It is important to obtain quantitative information to optimize the hemodynamic design of the CP connection.

The objective of this study was to quantify and qualify the flow fields and pressure loss of the CP connection in the models by using flow visualization techniques and pressure measurements. The results of this study of the complicated flow characteristics in the CP connection could help provide information about the optimal surgical methods used to correct these congenital heart defects.

MATERIALS AND METHODS

To understand the local fluid dynamics for different designs of the CP connection, five models were made out of Pyrex glass to facilitate in vitro study. The models consisted of the SVC, IVC, RPA and the left pulmonary artery (LPA). Fig. 1 shows a schematic drawing of Model I. The diameter of the model was determined based on the post-operative data of a four-year-old patient. Fig. 2 shows the other models with different geometric parameters. Models I, II and III have the same position as the center of the anastomosis of the IVC with that of the SVC, but Models IV and V have 10 mm offset

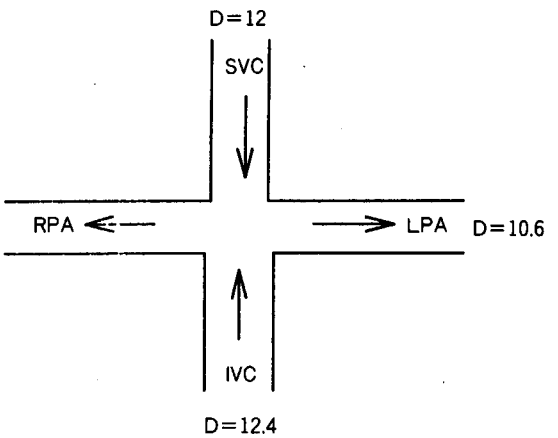

Fig. 1. Size and geometry of Model I.

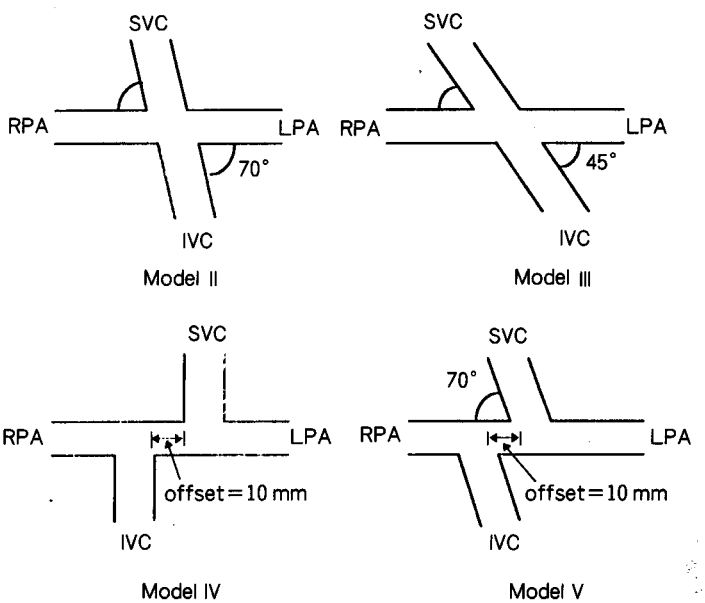

Fig. 2. Geometry of Model II, III, IV and V.

between them. Also, the anastomotic junction angles are different (Models I and IV: 90°, Models II and V: 70°, Model III: 45°). These models were then connected to a flow loop for flow visualization study. The schematic of the steady flow system is shown in Fig. 3. The exit was drained into a common fluid reservoir. The fluid was returned from this reservoir to a couple of constant-head tanks using a steady flow pump. From these tanks, the fluid flowed through two polyethylene tubes connected to the IVC and SVC of the models. The RPA and LPA of the models were also connected to two polyethylene tubes which returned the fluid to the reservoir. Therefore, the inlet and outlet flows of the model could be controlled individually. Water-glycerin solutions were used as a blood-analog fluid. At room temperature the fluid had a density and viscosity of 1.10 g/cc and 3.5 cP, respectively. Flow rates of 2 and 3 L/min were controlled by using resistances on the tube and 1/3 of the total flow passed through the SVC and 2/3 passed through the IVC. The flow rates were measured by placing the rotameters inline proximal to the IVC and SVC, and distal to the RPA. For flow visualization study, spherical Amberlite particles sized 50-200 μm were added to the blood analog fluid and illuminated with two 60W white lights. The flow streaklines were obtained by photographing the models using a 35 mm camera.

For a quantitative evaluation of the path of the particles through the models, the particles were added only to the IVC, and then the amount of particles coming out of the RPA and LPA was measured after drying the particles completely. Each experiment was repeated three times for each model. The flow streaklines coming out of the IVC were photographed to analyze the flow distribution in the models. The experiments were conducted at a total flow rate of 2 and 3 L/min.

The pressure drop across each model was obtained to determine the flow dynamic efficiency of the model based on each geometric configuration. The pressure was measured from the taps on each model's inlet and outlet. The positions of the taps on Model I are shown in Fig. 2. All taps were positioned at the midsection of the conduit, 50 mm from the conduit junction. Each measurement was repeated three times at the same model. The experiments were conducted at the total flow rate of 2 and 3 L/min.

RESULTS

The flow visualization study was conducted only at the total flow rate of 2L/min because there was no significant difference in flow pattern by varying the flow rate in this experiment. From the flow visualization study, the form and movement of flow

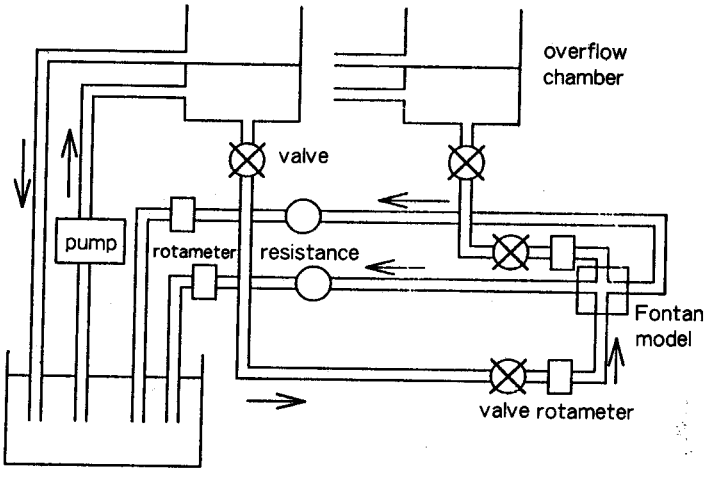

Fig. 3. In vitro steady flow system.

patterns were best observed in real time. In Model I, flows from the IVC and SVC were mixed in the middle of the junction (Fig. 4a) and turned toward the RPA and LPA after dividing evenly in half (Fig. 4b). No dominant vortex was seen in the central region of the junction, but a very unstable fluid mixture was created. The swirling caused by the mixture continued as it flowed through the RPA and LPA. In Model II, an unstable vortex was created (Fig. 5a). This vortex covered the central region of the junction without any stagnation regions. The flows from the IVC and SVC were separated just after changing their direction so that small stagnation zones were created at the starting points of the RPA and LPA. The flows from the IVC turned dominantly toward the LPA (Fig. 5b). In Model III, the flow patterns were very similar to those of Model II (Fig. 6a). A large vortex, greater than that of Model II, covered the entire region of the junction. The flow from the IVC turned more dominantly toward the LPA than it did for Model II (Fig. 6b). In both Models IV and V, a significant stagnation region was created in the middle of the offset region (Fig. 7, Fig. 8). The flows from the IVC turned dominantly toward the RPA in both models. Especially in Model V, the flow was very stable and most of the flow from the IVC turned toward the RPA.

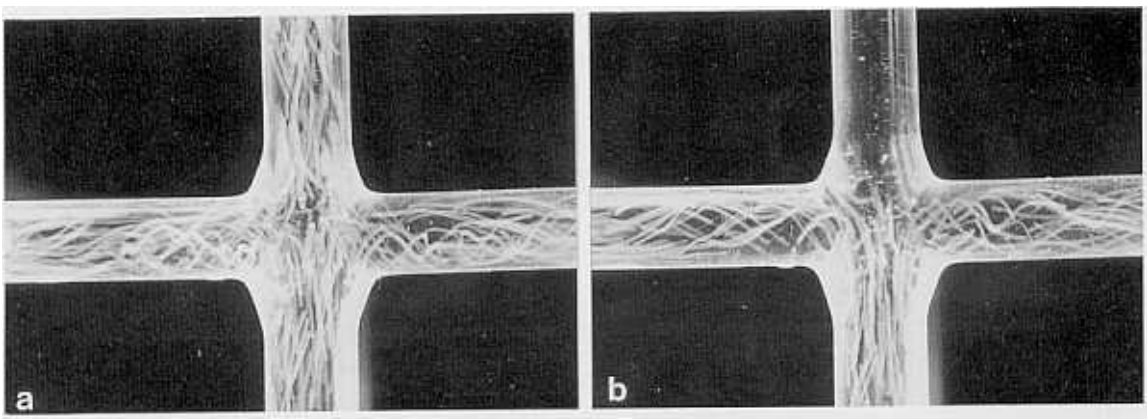

Fig. 4. Flow patterns in Model I: (a) when particles added into the IVC and SVC; (b) when particles added into IVC only.

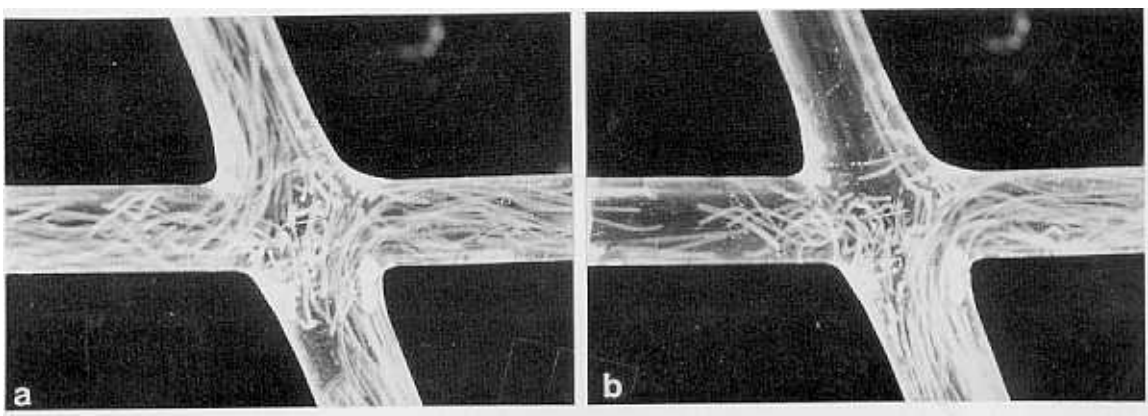

Fig. 5. Flow patterns in Model II: (a) when particles added into the IVC and SVC; (b) when particles added into IVC only.

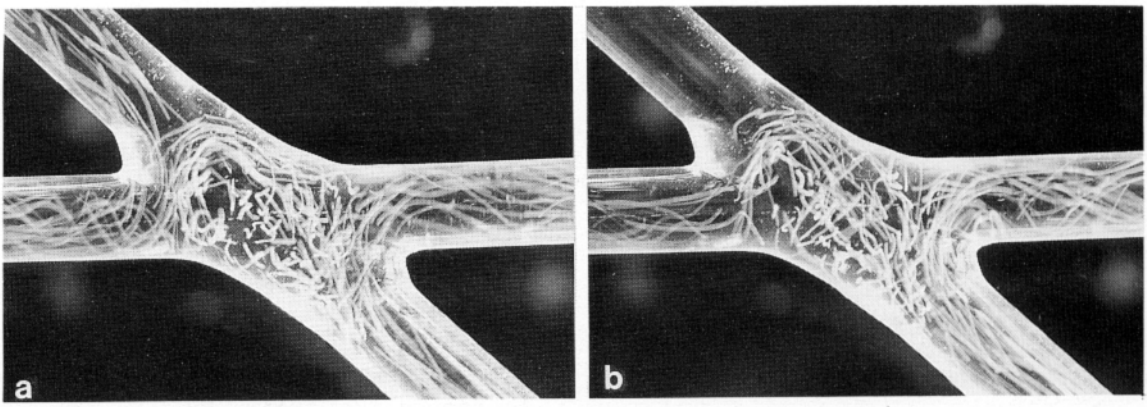

Fig. 6. *Flow patterns in Model III: (a) when particles added into the IVC and SVC; (b) when particles added into IVC only.*

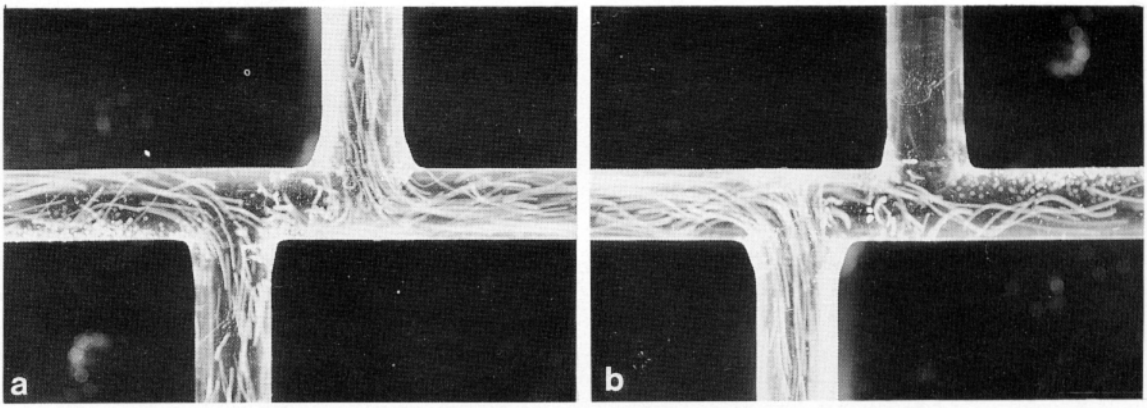

Fig. 7. *Flow patterns in Model IV: (a) when particles added into the IVC and SVC; (b) when particles added into IVC only.*

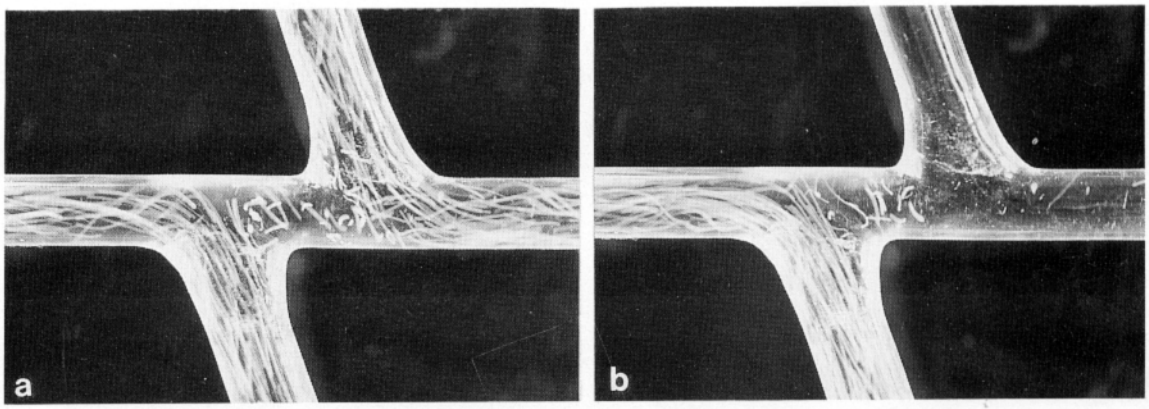

Fig. 8. *Flow patterns in Model V: (a) when particles added into the IVC and SVC; (b) when particles added into IVC only.*

Table 1 shows the results of weighing the particles coming out from the LPA and RPA after adding particles into the IVC to evaluate the quantitative path of the particles through the models. In Model I, as shown in Fig. 4b, both flows from the IVC and SVC turned evenly toward the RPA and LPA. In Model II, 62% of the flow from the IVC turned toward the LPA at the total flow rate of 2L/min. The unbalanced flow became greater in Model II, where the anastomotic junction angle was increased. Total flow rate was not a significant factor in determining the flow distribution of the models. The opposite flow ratios from Models II and III were obtained in Models IV and V. Most of the flow from the SVC turned toward the LPA in Models IV and V.

Table 1. The percentage of flow from the SVC and IVC toward the LPA and RPA

Model No.		From IVC		From SVC	
		2L/min	3L/min	2L/min	3L/min
I	LPA	50	50	50	50
	RPA	50	50	50	50
II	LPA	62	61	26	28
	RPA	38	39	74	72
III	LPA	71	69	8	12
	RPA	29	31	92	88
IV	LPA	22	23	100	100
	RPA	78	77	0	0
V	LPA	23	23	100	100
	RPA	77	77	0	0

The pressure measured at the inlet and outlet sections of the models are shown in Table 2. Generally, as the total flow rates increased from 2 to 3 L/min, the pressure in the models increased. The pressure in the LPA and RPA was greatest in Model IV.

DISCUSSION

In this paper the results of flow visualization study, flow distribution and pressure measurements in five types of CP connections are presented. This experiment extended previous results (de Leval *et al.* 1988; Low *et al.* 1992; Kim *et al.* 1995; Dubini *et al.* 1996) by using a greater variety of flow models to obtain quantitative information to help optimize the hemodynamic design of the CP connection. The flow pulsation effects were negligible since the right atrium and ventricle are totally bypassed and the inlet flows are from venous districts. As a consequence, the rigid wall of the models could be thought reasonable.

Table 2. The pressures (mmHg) measured in the models

Model No.	Position / Flow rate(L/min)	IVC (mmHg)	SVC (mmHg)	RPA (mmHg)	LPA (mmHg)
I	2	10.0	2.9	5.8	5.9
	3	12.6	5.6	8.5	8.5
II	2	13.1	6.3	9.2	9.2
	3	16.2	9.6	11.7	11.7
III	2	12.2	6.8	9.0	9.4
	3	14.6	9.4	11.6	11.5
IV	2	14.7	6.9	10.2	10.3
	3	18.0	10.4	13.2	13.4
V	2	11.7	4.5	7.4	7.7
	3	15.0	5.0	9.5	9.9

Flow visualization studies showed a highly swirling flow pattern in the LPA and RPA of Models I, II and III. The mixing of the two opposing flows in Model I created several small swirls in the middle of the model. The mixing in Models II and III developed to form a large vortex at the center of the anastomotic junction. The momentum imparted to the fluid by the vortex was carried with the fluid as it left the junction through the LPA and RPA. The severe mixing caused fluid energy loss as was observed in the models. In addition to the fluid energy loss due to viscous dissipation caused by the swirling, there were further energy losses due to a pressure drop caused by the increase in mixing associated with opposing flows. As shown in Table 2, there was little difference in pressure between Models II and III. That is because of the similarity in their design, except that the anastomotic junction angle is different for both models. But larger energy losses were expected in comparison to with Model I. The flow ratio of the IVC to the LPA was greater than that to the RPA in Models II and III. The flow patterns in Models IV and V showed that the flow ratio of the IVC to the LPA and RPA highly depended on the offset of the junction rather than on the anastomotic junction angle. Table 2 shows the pressure differences between the IVC and SVC were minimal, but that the pressure in the RPA and LPA had wide variations by changing the geometry of the model. This suggested that the geometry designed for this study had no significant effect on the pressure drop in the RPA and LPA. In addition to the reduction in energy losses, a correct pulmonary flow balance is important because an unbalanced flow distribution may cause severe damage to the lungs. Considering that the oxgen-exchange performance of the left lung is better than the right, and that IVC flow is twice that of SVC flow, physiologically it is desirable that more IVC flow should turn toward the RPA. Model V is best suited to this physiological condition, but the stagnation zone created in the offset should be reduced by shortening the length of the offset.

REFERENCES

De Leval MR, Kilner P, Gewillig M, Bull C : Total cavopulmonary connection: A logical alternative to atriopulmonary connection for complex Fontan operations. *J Thorac Cardiovasc Surg 96: 682- 695, 1988*

Dubini G, de Leval MR, Pietrabissa R, Montevecchi FM, Fumero R: A numerical fluid mechanical study of repaired congenital heart defects. Application to the total cavopulmonary connection. *J Biomech 29: 111-121, 1996*

Fontan F, Baudet E: Surgical repair of tricuspid atresia. *Thorax 26: 240-248, 1971*

Frommelt PC, Snider AR, Meliones JN, Vermilion RP: Doppler assessment of pulmonary artery flow patterns and ventricular function after the Fontan operation. *Am J Cardiol 68: 1211-1215, 1991*

Kim YH, Walker PG, Fontaine AA, Panchal S, Ensley AE, Oshinski J, Sharma S, Ha B, Lucas CL, Yoganathan AP: Hemodynamics of the Fontan connection: An in vitro study. *J Biomed Eng 117: 423-428, 1995*

Kobayashi J, Matsuda H, Nakano S, Shimazaki Y, Ikawa S, Mitsuno M, Takahashi Y, Kawashima Y, Arisawa J, Matsushita T: Hemodynamic effects of bidirectional cavopulmonary shunt with pulsatile pulmonary flow. *Circulation 84 (Suppl III): 219-225, 1991*

Low HT, Chew YT, Lee CN: *Flow studies on the Fontan surgical connections.* Singapore, 7th International Conference on Biomedical Engineering, *Dec. 2-4, 1992*

Nakazawa M, Nojima K, Okuda H, Imai Y, Nakanishi T, Kurosawa H, Takao A: Flow dynamics in the main pulmonary artery after the Fontan procedure in patients with tricuspid atresia or single ventricle. *Circulation 75: 1117-1123, 1987*

Penny DJ, Redington AN: Doppler echocardiographic evaluation of pulmonary blood flow after the Fontan operation: the role of the lungs. *Br Heart J 66: 372-374, 1991*

Rebergen SA, Ottenkamp J, Doornbos J, van der Wall EE, Chin JGJ, de Roos A: Postoperative pulmonary flow dynamics after Fontan surgery: Assessment with nuclear magnetic resonance velocity mapping. *J Am Coll Cardiol 21: 123-131, 1993*